

Inhibited Feshbach Conversion of Atomic Fermions to Molecular Bosons due to Particle Interactions

Jie Liu,¹ Li-Bin Fu,¹ Bin Liu,^{1,2} Shi-Ping Yang,² and Biao Wu³

¹*Institute of Applied Physics and Computational Mathematics, Beijing, 100088, China*

²*Department of Physics, Hebei Normal University, Shijiazhuang 050016, China*

³*Institute of Physics, Chinese Academy of Sciences, P.O.Box 603, Beijing 100080, China*

We investigate the dynamics for Feshbach Conversion of Atomic Fermions to Molecular Bosons and show that the repulsive interaction between bosonic molecules enhances the conversion efficiency whereas the repulsive fermion atomic interaction and atom-molecule interaction suppress the conversion efficiency. The sum of the above interactions could lead to a ceiling for the atom-molecule conversion rate. Our model predicts a nonmonotonous dependence of the conversion rate on mean atomic density. Our results agrees with existing experimental data on ⁶Li and ⁴⁰K.

PACS numbers: 03.75.Ss, 05.30.Fk, 05.30.Jp, 03.75.Mn

Feshbach resonance has now become a focal point of the research activities in cold atom physics[1, 2, 3, 4] since its first experimental realization with the sodium atomic gas[5]. Among these research activities, the production of diatomic molecules from Fermi atoms with Feshbach resonance is of special interest and has attracted great attention. First, it is an interesting phenomenon by itself; second, it has applications ranging from the search for the permanent electric dipole moment[6] to providing unique experimental access to the BCS-BEC crossover physics[7]. So far, by slowly sweeping the magnetic field through the Feshbach resonance, samples of over 10^5 very weakly bound molecules (binding energy ~ 10 kHz) at temperatures of a few tens of nK have been produced from quantum degenerate Fermi gas[8, 9, 10].

In all these experiments people observed one common and intriguing phenomenon, a ceiling of less than 100% on the conversion efficiency in the adiabatic limit. If one uses the standard Landau-Zener(LZ) model[11] to describe this Feshbach conversion, one would predict 100% molecular conversion for sufficiently slow sweeps and an exponential dependence of the efficiency on the sweep rate. This intriguing finding immediately caught the attention of theorists. Various models have been proposed[12, 13, 14]; however, many of these theories[12, 13, 14, 15] can not account for the ceiling phenomenon. By far, there are two theories explaining the ceiling phenomenon[16, 17]. Both of them attribute it to statistical mixture of two spin states and predict a 50% ceiling. However, the recent data on ⁴⁰K showed a high conversion efficiency up to 90% at a low temperature of $T/T_F = 0.05$ [15]. In Ref.[17], this high conversion was speculated to be due to multiple collisions.

In this letter we show that the repulsive interactions between the particles including atom-atom, molecule and atom-molecule, which is ignored in all previous theoretical works[12, 13, 14, 16, 17], can suppress the conversion efficiency from atomic fermions to molecules and cause the ceiling phenomenon. This interaction-suppressed conversion efficiency is in spirit the same as

the broken-adiabaticity by interaction in the nonlinear LZ tunneling[18, 19]. Furthermore, in contrary to the LZ theory widely used to account for atom-molecule conversion[4], our model predicts a nonmonotonous dependence of the conversion rate on mean atomic density due to the interactions between particles. Our theory has been compared to the recent experiments with ⁶Li and ⁴⁰K[9, 15]. They are in good agreement.

We extend the two channel model[20, 21, 22] to include the particle interactions and write the system Hamiltonian as,

$$\begin{aligned}
 H = & \sum_{\mathbf{k},\sigma} \epsilon_{\mathbf{k}} a_{\mathbf{k},\sigma}^\dagger a_{\mathbf{k},\sigma} + \left(\gamma + \frac{\epsilon_b}{2} \right) b^\dagger b \\
 & + \frac{U_a}{V_a} \sum_{\mathbf{k},\mathbf{k}'} a_{\mathbf{k},\uparrow}^\dagger a_{-\mathbf{k},\downarrow}^\dagger a_{-\mathbf{k}',\downarrow} a_{\mathbf{k}',\uparrow} \\
 & + \frac{U_{ab}}{V_a} \sum_{\mathbf{k},\sigma} a_{\mathbf{k},\sigma}^\dagger a_{\mathbf{k},\sigma} b^\dagger b + \frac{U_b}{V_b} b^\dagger b^\dagger b b \\
 & + \frac{g\sqrt{V_b}}{V_a} \sum_{\mathbf{k}} \left(b^\dagger a_{-\mathbf{k},\downarrow} a_{\mathbf{k},\uparrow} + a_{\mathbf{k},\uparrow}^\dagger a_{-\mathbf{k},\downarrow}^\dagger b \right). \quad (1)
 \end{aligned}$$

Here $\epsilon_{\mathbf{k}} = \hbar^2 k^2 / 2m_a$ is the kinetic energy of the atom and $\sigma = \uparrow, \downarrow$ denotes the two hyperfine states of the atom. $U_a = \Lambda U_0, U_{ab} = \Lambda U_1, g = \Lambda g_0$, and $\gamma = \gamma_0 - \Lambda g_0^2 / U_c$, where $\gamma_0 = \mu_{co}(B - B_0)$ is the molecule energy under the linearly changing magnetic field with $B = -\alpha_r t$, $g_0 = \sqrt{4\pi\hbar^2 a_{bg} \Delta B \mu_{co} / m_a}$ is the atom-molecule coupling [3], $U_0 = 4\pi\hbar^2 a_{bg} / m_a$ is the interaction between atoms, $U_1 = 4\pi\hbar^2 1.2 a_{bg} / m_{ab}$ is the atom-dimer scattering interaction, and $U_b = 4\pi\hbar^2 0.6 a_{bg} / m_b$ is the interaction between molecules[23]. $\Lambda \equiv (1 + U_0/U_c)^{-1}$ and $U_c^{-1} = -\sum_{\mathbf{k}} (\exp(-k^2/k_c^2) / 2\epsilon_{\mathbf{k}})$ with the cutoff momentum k_c representing the inverse range of interaction [22, 24, 25]. B_0 and ΔB are Feshbach resonance point and width, respectively. m_a and $m_b = 2m_a$ are masses for atoms and molecules, and accordingly $m_{ab} = \frac{2}{3}m_a$ is the reduced mass for the atom-dimer interaction.

Due to the magnetic trap used in current experiments, the molecular bosons are more tightly confined in space

than the fermionic atoms, so in the above Hamiltonian we use two characters V_a and V_b to symbol the volumes of bosonic atoms and fermionic molecules, respectively. We also assume the zero temperature limit so that only one bosonic mode needs to be considered and ignore all possible dissipations in the system, such as the loss of atoms by three-body collision.

In current experiments, the intrinsic energy width of a Feshbach resonance is much larger than the Fermi energy E_F [26], it is therefore reasonable to make the approximation $\epsilon_{\mathbf{k}} = \epsilon$, which is called degenerate model in Ref.[12, 13, 21]. We introduce the following operators[12, 13], $L_x = \frac{\sum_{\mathbf{k}}(a_{\mathbf{k},\uparrow}^\dagger a_{-\mathbf{k},\downarrow}^\dagger b + b^\dagger a_{-\mathbf{k},\downarrow} a_{\mathbf{k},\uparrow})}{(N/2)^{3/2}}$, $L_y = \frac{\sum_{\mathbf{k}}(a_{\mathbf{k},\uparrow}^\dagger a_{-\mathbf{k},\downarrow}^\dagger b - b^\dagger a_{-\mathbf{k},\downarrow} a_{\mathbf{k},\uparrow})}{i(N/2)^{3/2}}$, $L_z = \frac{\sum_{\mathbf{k},\sigma} a_{\mathbf{k},\sigma}^\dagger a_{\mathbf{k},\sigma} - 2b^\dagger b}{N}$, where $N = 2b^\dagger b + \sum_{\mathbf{k},\sigma} a_{\mathbf{k},\sigma}^\dagger a_{\mathbf{k},\sigma}$ is the conserved total number of particles. With the commutators $[L_z, L_x] = \frac{4i}{N}L_y$, $[L_z, L_y] = -\frac{4i}{N}L_x$, $[L_x, L_y] = \frac{i}{N}(1 - L_z)(1 + 3L_z) + o(1/N^2)$, we can obtain the Heisenberg equations for the system $i\hbar \frac{d}{dt}L_l = [L_l, H]$, $l = x, y, z$, $H = \frac{N}{4} \left(2\epsilon - (\gamma + \frac{\epsilon_b}{2}) - \frac{NU_a}{2V_a} - \frac{NU_{ab}}{V_a} \right) L_z - \frac{N^2}{16} \left(\frac{U_a}{V_a} + \frac{2U_{ab}}{V_a} - \frac{U_b}{V_b} \right) (1 - L_z)^2 + \frac{g}{\sqrt{V_a}} \left(\frac{N}{2} \right)^{3/2} L_x$ [27]. Since all the commutators vanish in the limit of $N \rightarrow \infty$ and N is large for the current experiments, it is appropriate to take L_x , L_y , and L_z as three real numbers u, v, w , respectively. With straightforward algebra, one can prove the identity $u^2 + v^2 = \frac{1}{2}(w - 1)^2(w + 1)$ and that these Heisenberg equations are reduced to

$$ds/d\tau = \sqrt{(1-s)^2(s+1)} \sin(\theta), \quad (2)$$

$$d\theta/d\tau = \delta - 2\chi(1-s) - \frac{1+3s}{2\sqrt{1+s}} \cos\theta, \quad (3)$$

where $s = w$, $\theta = \arctan(v/u)$, $\tau = gt\sqrt{NV_b}/\hbar V_a$, $\delta = \left(2\epsilon - (\gamma + \frac{\epsilon_b}{2}) - \frac{NU_a}{2V_a} - \frac{NU_{ab}}{V_a} \right) V_a/g\sqrt{NV_b}$, $\chi = \left(U_a + 2U_{ab} - \frac{U_b V_a}{V_b} \right) \sqrt{N}/4g\sqrt{V_b}$. By a trivial shift of time origin, we can set $\delta = \alpha\tau$ and mean atomic density $n = N/V_a$. Note that s and θ are a pair of conjugate canonical variables and Eqs.(2,3) are equations of motion of the following Hamiltonian ,

$$\mathcal{H} = \delta s - \chi(1-s)^2 + \sqrt{(1+s)(1-s)^2} \cos\theta. \quad (4)$$

These approximations and simplifications show that all the experimental parameters affect the system via only two dimensionless parameters, effective sweeping rate α and nonlinear parameter χ , which are given by

$$\frac{\alpha_r}{\alpha} = \frac{4\pi\hbar n a_{bg} \Delta B}{m_a} \Lambda^2 \frac{V_b}{V_a}, \quad (5)$$

$$\chi = \left(2.3 - \frac{0.15V_a}{\Lambda V_b} \right) \sqrt{\frac{V_a}{V_b}} \sqrt{\frac{\pi\hbar^2 a_{bg} n}{m_a \mu_{co} \Delta B}}. \quad (6)$$

To understand the dynamics, we first look at the fixed points $\dot{s} = 0, \dot{\theta} = 0$ of the above classical Hamiltonian.

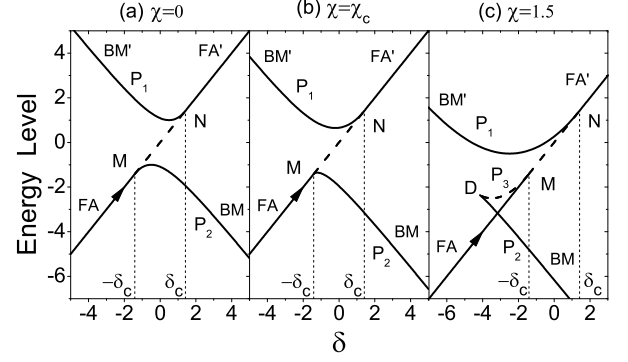


FIG. 1: Adiabatic energy levels for different interaction strengths. (a) $\chi = 0$; (b) $\chi = \chi_c = \sqrt{2}/4$; (c) $\chi = 1.5$. $\delta_c = \sqrt{2}$. The states denoted by dashed segments MN and DM are unstable.

The energies for these fixed points make up energy levels of the system as shown in Fig.1. One sees that the structure of these energy levels changes dramatically as the molecular interaction strength χ increases. When χ is beyond the critical value $\chi_c = \sqrt{2}/4$, there appears a loop in the energy levels. As we shall see, this loop has highly non-trivial physical consequences. Some features in Fig.1: (i) There are two fixed points when $|\delta|$ is large enough: one for bosonic molecule (BM) and the other for fermionic atom (FA). (ii) When $|\delta| < \sqrt{2}$, there is an additional fixed point with $s = 1$. However, this fixed point is unstable[28]. (iii) For $\chi > \chi_c$, there appears one more fixed point denoted by P_3 and, consequently, a loop in the energy levels. This P_3 fixed point is also unstable. Dashed lines are used for unstable fixed points in Fig.1.

Consider now the adiabatic evolution of the system starting from the high negative value of δ with $s = 1$. This corresponds to the experiments where the magnetic field sweeps slowly across the Feshbach resonance with no bosonic molecules initially. When χ is small, such as in Fig.1(a), the system's evolution will simply follow the solid line, converting all fermionic atoms into molecules. However, when χ is beyond χ_c as in Fig.1(c), the system will find no stable energy level to follow at singular point N. As a result, only a fraction of fermionic atoms are combined into molecules. This simple analysis is confirmed by our numerical results, which are plotted in Fig.2. In our calculation, the 4-5th Runge-Kutta step-adaptive algorithm is used in solving the differential equations (2,3). Because $s = 1$ is a fixed point when $\delta < -\sqrt{2}$, we start from $s \simeq 1, \theta = \pi$ and sweep the field from $\delta = -\sqrt{2}$ to 200. In Fig.2, the fraction Γ of remnant fermionic atoms is drawn as a function of α . It is evident that Γ approaches zero as $\alpha \rightarrow 0$ when $\chi < \chi_c$, indicating that all atoms are converted into molecules in the adiabatic limit. In contrast, when $\chi > \chi_c$, Γ does not decrease to zero as $\alpha \rightarrow 0$. Moreover, our numerical results show

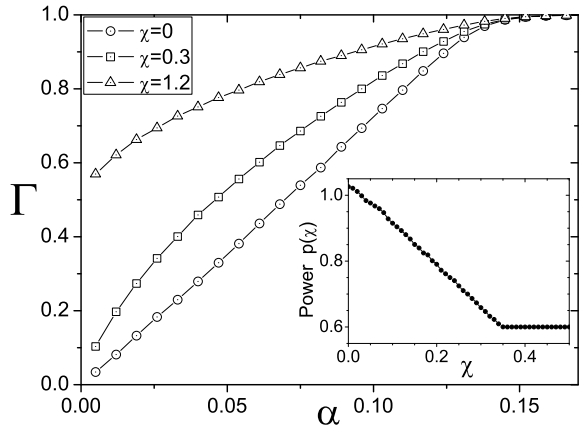


FIG. 2: Fraction Γ of remnant fermionic atoms as a function of the sweeping rate α . This function is a power of α with the power depending on χ . The power $p(\chi)$ is shown in the inset.

that Γ has a power-law dependence on the sweeping rate α ,

$$\Gamma \propto \alpha^{p(\chi)}, \quad (7)$$

very different from the standard LZ model where Γ would be an exponential function of α . Further analysis finds that the power p is a function of the molecular interaction strength χ . As shown in the inset of Fig.2, $p(\chi)$ decreases from one to 3/5 and becomes a constant of 3/5 beyond $\chi = \chi_c$.

In the adiabatic limit, we have shown that there is a nonzero fraction Γ_{ad} of non-converted atoms when the molecular interaction χ is large enough. To learn how this fraction Γ_{ad} depends on χ , we turn to the phase space diagrams of our system as shown in Fig.3. We focus first on the first row of this figure. As δ ramps up slowly from a large negative value, the fixed point branches into two fixed points at $\delta = -\sqrt{2}$: one is unstable, corresponding to the dashed MN line in Fig.1; the other is the stable elliptic fixed point P_2 . As δ further increases slowly, the system follows the evolution of P_2 and the atoms converts 100% into molecules.

The situation becomes very different for the second row of Fig.3, where $\chi = 0.6 > \chi_c$. As soon as the fixed point appearing at $s = 1$ when $\delta = -\sqrt{2}$, it merges with a hyperbolic fixed point P_3 . More interestingly, it is no longer a fixed point and will evolve along the dark line in Fig.3(e). The dark line is given by $\sqrt{2} = \chi(1-s) - \sqrt{1+s \cos \theta}$, which is found by taking $E = \delta = -\sqrt{2}$ into the classical Hamiltonian (4). As the action of this trajectory is nonzero while a fixed point has zero action, this merger of two fixed points represents a sudden jump in action. It is this sudden jump that has caused the nonzero fraction of remnant atoms. As δ ramps up further slowly, the trajectory will change

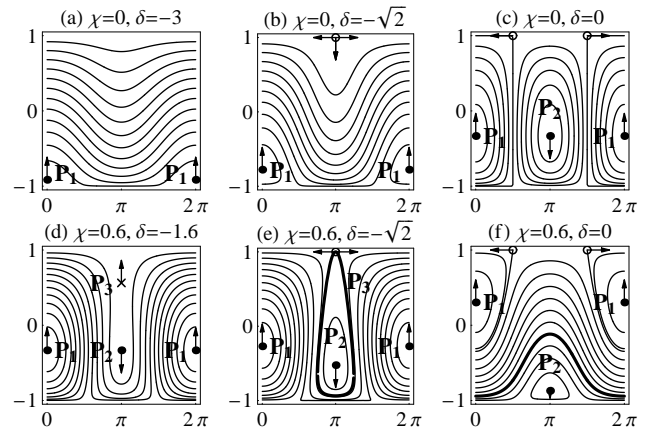


FIG. 3: Phase spaces of Hamiltonian (4). The two fixed points on line $s = 1$ in (c) and (f) are in fact the same fixed point in terms of u, v, w ; they are artifact caused by the definition $\theta = \arctan(v/u)$.

its shape as witnessed in Fig.3(f); however, its action stays constant as demanded by the classical adiabatic theorem[29, 30]. The action is

$$I = \begin{cases} \frac{1}{2\pi} \oint \frac{\cos \theta \sqrt{8\chi^2 - 4\sqrt{2}\chi + \cos^2 \theta}}{2\chi^2} d\theta, & \frac{\sqrt{2}}{4} < \chi < \frac{\sqrt{2}}{2}; \\ \frac{1}{2\pi} \int_0^{2\pi} \frac{4\chi^2 - 2\sqrt{2}\chi + \cos^2 \theta}{2\chi^2} d\theta, & \chi > \frac{\sqrt{2}}{2}, \end{cases} \quad (8)$$

which gives the fraction of remnant fermionic atoms as

$$\Gamma_{ad} = \frac{1}{2}I = 1 - \frac{4\sqrt{2}\chi - 1}{8\chi^2}. \quad (9)$$

For the rapid sweeping field, we find an exponential dependence of the remnant fraction of unconverted atoms on the sweeping rates, i.e., $\ln \Gamma \propto \frac{1}{\alpha}$, with a modified prefactor compared to the standard Landau-Zener formula due to the emergence of the interaction parameter.

The above calculations show that positive χ suppresses the conversion efficiency whereas the negative χ enhances it. Because the repulsive interaction between bosonic molecules contributes a negative quantity to χ therefore enhancing the conversion efficiency; the repulsive fermion atomic interaction and atom-molecule interaction contributes a positive quantity to χ therefore suppressing the conversion efficiency.

Now we compare our theory with existing experiments. For the experiment with ${}^6\text{Li}$ [9], the mean density is $n = 4 \times 10^{12} \text{cm}^{-3}$ with $N = 6 \times 10^5$ atoms. The scatter length $a_{bg} = 59a_B$, $\mu_{co} \sim 2\mu_B$, where a_B and μ_B are Bohr radius and Bohr magneton, respectively, and the resonance width $\Delta B = 0.1G$ at $B_0 = 543.8G$. From Eq.(6), we find the interaction parameter as $\chi = 1.16$, which in turn gives us a ceiling of $\Gamma_{ad} = 0.49$ via Eq.(9). This is in good agreement with experiment. In addition, we have calculated numerically the conversion efficiency as a function of sweeping rates. To compare with experiment, we need to calculate the renormalization factor Λ .

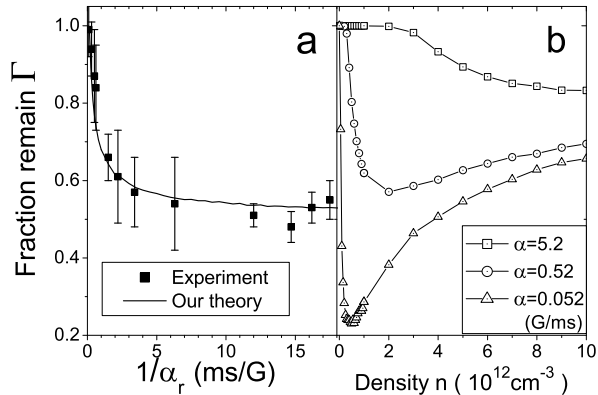


FIG. 4: (a) Comparison between theory and experimental data of ${}^6\text{Li}$ [9]. Γ is the fraction of unconverted fermionic atoms, α_r is the field sweep rate; (b) Our model calculation predicts the dependence of Γ on mean atomic density.

Fermi energy $E_F = \hbar^2 k_F^2 / 2m \approx 1.4\mu\text{K}$ for ${}^6\text{Li}$, we set $V_a/V_b = 2000$ and $\Lambda = 500$ with using a momentum cut-off $K_c = 96k_F$ [31]. The comparison between our theory and experiment is shown in Fig.4. Moreover, our model predicts a nonmonotonous dependence of the conversion rate on mean atomic density (see Fig.4b). This can be understood from our Eq.(5-6). In Eq.(5), we see the effective sweeping rate α is inversely proportional to the atomic density, so increasing the density will reduce the effective sweeping rate and therefore enhance the conversion rate. On the other hand, higher density will give larger nonlinearity χ as indicated by Eq.(6), which in turn suppresses the atom-molecule conversion. These two factors compete with each other giving rise to the nonmonotonous curves in Fig.4b. In practical experiments,

to achieve higher conversion efficiency, one need carefully choose initial fermionic atom density making it fall into the optimal parameter regime.

For ${}^{40}\text{K}$, the situation is different. The resonance at $B_0 = 202.1\text{G}$ has a large width of $\Delta B = 7.8\text{G}$ and the mass of ${}^{40}\text{K}$ is 7 times that of ${}^6\text{Li}$. With $a_{bg} = 174a_B$, $\mu_{co} \sim 2\mu_B$, initial clouds have mean densities ranging from 2×10^{12} to $4 \times 10^{13}\text{cm}^{-3}$, and $N = 2.5 \times 10^5 \sim 1.5 \times 10^6$ [15], then the interaction parameter χ falls into the interval $[0.04, 0.47]$, which predicts a molecular conversion ranging from 94% to 100%. Indeed, conversion efficiency up to 90% has been observed[15].

We emphasize that the suppressed conversion efficiency by particle interaction dominates only at low temperatures. As a result, in the above we have only compared to the data obtained at low temperatures ($T/T_F = 0.1$ for ${}^6\text{Li}$ and $T/T_F = 0.05$ for ${}^{40}\text{K}$). Temperature can affect the conversion efficiency strongly as shown in Ref. [15]. The ceiling of 50% conversion efficiency observed in Ref.[8] is likely a thermal effect since the experiment is performed at $T/T_F = 0.33$.

In summary, we have investigated the Feshbach conversion of atomic fermions to molecular bosons and show that the interactions between particles plays a vital role: When the dimensionless interaction parameter χ is large enough, the conversion efficiency is dramatically suppressed. When χ is small, the conversion efficiency is expected to be 100% for adiabatic sweeping magnetic fields. Our theory is consistent with the existing data. Our model predicts a nonmonotonous dependence of the conversion rate on mean atomic density.

This work was supported by NSF of China (10474008,10604009,10504040) and the 973 project (2005CB724500,2006CB921400). B.W. is also supported by the ‘‘BaiRen’’ program of the Chinese Academy of Sciences.

-
- [1] E. Timmermans, P. Tommasini, M. Hussein, and A. Kerman, *Phys. Rep.* **315**, 199 (1999).
[2] R. A. Duine and H.T.C. Stoof, *Phys. Rep.* **396**, 115 (2004).
[3] Q.J. Chen, J. Stajic, S.N. Tan, and K. Levin, *Phys. Rep.* **412**, 1 (2005).
[4] T. Köhler, K. Góral, and P.S. Julienne, *Rev. Mod. Phys.* **78**, 1311 (2006).
[5] S. Inouye, M.R. Andrews, J. Stenger, H.-J. Miesner, D.M. Stamper-Kurn, and W. Ketterle, *Nature* **392**, 151 (1998).
[6] J. J. Hudson et al., *Phys. Rev. Lett.* **89**, 23003 (2002).
[7] C.A. Regal, M. Greiner, and D.S. Jin, *Phys. Rev. Lett.* **92**, 040403 (2004).
[8] C. A. Regal et al., *Nature (London)* **424**, 47 (2003).
[9] K.E. Strecker, G.B. Partridge, and R.G. Hulet, *Phys. Rev. Lett.* **91**, 080406 (2003).
[10] J. Cubizolles et al., *Phys. Rev. Lett.* **91**, 240401 (2003).
[11] C. Zener, *Proc. R. Soc. A* **137**, 696 (1932); L. D. Landau and E. M. Lifshitz, *Quantum Mechanics* (Pergamon, Oxford, 1977).
[12] E. Pazy, I. Tikhonenkov, Y. B. Band, M. Fleischhauer, and A. Vardi, *Phys. Rev. Lett.* **95**, 170403 (2005).
[13] I. Tikhonenkov, E. Pazy, Y. B. Band, M. Fleischhauer, and A. Vardi, *Phys. Rev. A* **73**, 043605 (2006).
[14] E. Altman and A. Vishwanath, *Phys. Rev. Lett.* **95**, 110404 (2005).
[15] E. Hodby, S. T. Thompson, C. A. Regal, M. Greiner, A. C. Wilson, D. S. Jin, E. A. Cornell, and C. E. Wieman, *Phys. Rev. Lett.* **94**, 120402 (2005).
[16] E. Pazy, A. Vardi, and Y. B. Band, *Phys. Rev. Lett.* **93**, 120409 (2004).
[17] J. Chwedeńczuk, K. Góral, T. Köhler, and P. S. Julienne, *Phys. Rev. Lett.* **93**, 260403 (2004).
[18] B. Wu and Q. Niu, *Phys. Rev. A* **61**, 023402 (2000).
[19] Jie Liu, Libin Fu, Bi-Yiao Ou, Shi-Gang Chen, Dae-II

- Choi, Biao Wu, and Qian Niu, Phys. Rev. A **66**, 023404 (2002).
- [20] J. Javanainen et al., Phys. Rev. Lett. **92**, 200402 (2004); R. A. Barankov and L. S. Levitov, Phys. Rev. Lett. **93**, 130403 (2004); A. V. Andreev et al., Phys. Rev. Lett. **93**, 130402 (2004); J. Dukelsky et al., Phys. Rev. Lett. **93**, 050403 (2004).
- [21] T. Miyakawa and P. Meystre, Phys. Rev. A **71**, 033624 (2005).
- [22] W. Yi and L.-M. Duan, Phys. Rev. A **73**, 063607 (2006).
- [23] Here, the a_{bg} of atom-dimer and molecule is taken to be 1.2 and 0.6 times that of the corresponding atoms respectively, see, D. S. Petrov, C. Salomon, and G. V. Shlyapnikov, Phys. Rev. Lett. **93**, 090404 (2004).
- [24] S. J. J. M. F. Kokkelmans, J. N. Milstein, M. L. Chiofalo, R. Walser, and M. J. Holland, Phys. Rev. A **65**, 053617 (2002).
- [25] Qijin Chen and K. Levin, Phys. Rev. Lett. **95**, 260406 (2005).
- [26] R.B. Diener and T.-L. Ho, cond-mat/0405174.
- [27] The deduction of scattering terms of the molecule- molecule and atom-molecule is straightforward. In deducing the atom-atom scattering term we need introduce the collective pseudo-spin operators $\hat{S}^+ = \sum_{\mathbf{k}} a_{\mathbf{k}\uparrow}^\dagger a_{-\mathbf{k}\downarrow}^\dagger$, $\hat{S}^- = \sum_{\mathbf{k}} a_{-\mathbf{k}\downarrow} a_{\mathbf{k}\uparrow}$, $\hat{S}_z = \sum_{\mathbf{k}} \frac{1}{2}(a_{\mathbf{k}\uparrow}^\dagger a_{\mathbf{k}\uparrow} + a_{-\mathbf{k}\downarrow}^\dagger a_{-\mathbf{k}\downarrow} - 1)$, It is easy to prove that $\hat{S}^2 = \hat{S}_z^2 - \hat{S}_z + \hat{S}^+ \hat{S}^-$ is a conservation and $S = N/4$. Combining the conserved relation of the total particles, $N/4 = \hat{b}^\dagger \hat{b} + \hat{S}_z$, we can rewrite the atom-atom scattering term as $\hat{S}^+ \hat{S}^- = \frac{1}{2} \sum_{\mathbf{k}, \sigma} a_{\mathbf{k}, \sigma}^\dagger a_{\mathbf{k}, \sigma} \hat{b}^\dagger \hat{b} + \frac{N}{2} - \hat{b}^\dagger \hat{b}$.
- [28] The stability of the fixed points is evaluated by calculating the eigenvalues of the linearized equations near the fixed points, see Ref.[19].
- [29] L. D. Landau and E. M. Lifshitz, Mechanics (Pergamon, Oxford, 1977).
- [30] Jie Liu, Biao Wu, and Qian Niu, Phys. Rev. Lett. **90**, 170404 (2003)
- [31] The cutoff k_c is such chosen that the tunnelling window $2\delta_c$ for converting atomic fermions to molecular bosons consists with Feshbach resonance width $\mu_{co}\Delta B$ of ${}^6\text{Li}$.